Measurement and Mapping of pH in Hydrating Pharmaceutical Pellets Using Confocal Laser Scanning Microscopy

Sandra J. Cope,[1] Stephen Hibberd, [2] Joanne Whetstone,[1] Ross J. MacRae, [3] and Colin D. Melia [1,4]

Received May 28, 2002; accepted July 1, 2002

Purpose. pH modifiers are often used to promote drug solubility/stability in dosage forms, but predicting the extent and duration of internal pH modification is difficult. Here, a noninvasive technique is developed for the spatial and temporal mapping of pH in a hydrated pharmaceutical pellet, within a pH range appropriate for microenvironmental pH control by weak acids.

Methods. Confocal dual excitation imaging (Ex 488/Ex 568) of pellets containing a single, soluble, pH-sensitive fluorophore with cross-validation from a pH microelectrode. The technique was used to investigate the changing pH distribution in hydrating pellets containing two weak acids of differing solubility.

Results. The algorithm developed provided pH measurements over the range pH 3.5-5.5 with a typical accuracy of 0.1 pH units and with excellent correlation with pH microelectrode measurements. The method showed how pellets containing 25%w/w tartaric acid exhibited a rapid but transient fall in internal pH, in contrast to a slower more prolonged reduction with fumaric acid.

Conclusions. Spatial and temporal monitoring of pH in pellets was achieved with good accuracy within a pH range appropriate to pH modification by weak acids. However, the method developed is also generic and with suitable fluorophores will be applicable to other pH ranges and other dosage forms.

KEY WORDS: pH measurement; confocal laser scanning microscopy; fluorescence; pellets; weak acids.

INTRODUCTION

The incorporation of pH-modifying excipients is a common strategy for improving the release of pH-dependent drugs from dosage forms in adverse pH environments. These excipients are intended, on hydration, to create a pH environment inside or around a dosage form that is favourable to drug dissolution. This is a common problem with weakly basic drugs that exhibit poor solubility at intestinal pH, and where addition of a soluble acidic modifier to the formulation may dramatically improve bioavailability (1–8). Although this approach is effective, at the present time formulation design is undertaken empirically as the extent and the duration of the pH-modifying effect cannot be properly measured or predicted. A first step to improving this situation is to develop methods that allow quantitative measurement of pH inside a hydrated dosage form, and an ability to make these measurements noninvasively would also be an advantage, as this would allow the time course of pH change to be monitored *in situ*. Spatially resolved mapping would be a further advantage, as the time course and distribution of pH modification within the hydrated dosage may be important. It can be envisaged that heterogeneity may arise from differences in water availability, component distributions, dissolution rates, and the changing concentration gradients within the dosage of drug and the pH modifier.

Few reports to date describe measurements of pH inside dosage forms. A pH microprobe has been used by Doherty *et al.* to measure the surface pH of a tablet during dissolution (9). Electron paramagnetic resonance (EPR) has been used to measure pH inside water-in-oil emulsions (10) and to monitor the acidic environment inside hydrolytically degrading poly(anhydride) polymers both *in vitro* and *in vivo*(11). However, in comparison to light-based microscopies, the spatial resolution of EPR is relatively poor.

The optical-sectioning capability of confocal laser scanning microscopy (CLSM) offers the potential for high-resolution spatial mapping of fluorescent markers and drugs. Cutts *et al.* (12) have shown how this technique may be used to image the changing distribution of a fluorescent drug (minocycline) inside hydrating pellets and how this data may be analyzed to provide estimates of internal drug dissolution and diffusion coefficients. There is an obvious extension of this work to the fluorimetric monitoring of other internal processes. For example, the pH-dependent fluorescent response of fluorescein has been used to monitor pH inside microparticles (13), but these measurements suffered from the lack of an internal standard, without which it is not possible to distinguish low pH from low fluorescein concentration. A more effective approach is ratiometry, in which two fluorophores are monitored, one of which provides an internal standard. Fu *et al.* (14) have utilised this strategy effectively; using the response of two internally immobilised fluorophores to monitor the pH distribution and kinetics of acidification inside degrading poly (lactide-co-glycolide) microspheres. The technique relies on incorporation of sufficient quantities of each fluorophore into the microsphere. A better situation, however, would be to use (i) a single rather than a mixture of fluorophores so that problems of separation arising from differing partition or diffusion properties of the fluorophores in the dosage form are avoided. And (ii) to use a fluorophore probe that is soluble in the hydration solution so that the internal pH of a dosage form may be probed without the need to prepare specially labeled fluorescent ingredients.

In cell biology, dual wavelength CLSM is routinely utilised to measure intracellular pH locally in tissues, cells, and organelles (15–24). However the water-rich, relatively low ionic strength environment in biologic material contrasts sharply with the heterogeneous low water environment potentially containing high concentrations of dissolved solids likely to be encountered within most hydrated- controlled

[1] Institute of Pharmaceutical Sciences Research, School of Pharmaceutical Sciences, University of Nottingham, University Park, Nottingham NG7 2RD United Kingdom.
[2] School of Mathematical Sciences, University of Nottingham, University Park, Nottingham NG7 2RD United Kingdom.
[3] Pharmaceutical R&D, Pfizer Global Research and Development, Pfizer Limited, Sittingbourne, Kent ME9 8AG United Kingdom.
[4] To whom correspondence should addressed. (e-mail: colin.melia@nottingham.ac.uk)

ABBREVIATIONS: CLSM, confocal laser scanning microscopy; SIF, simulated intestinal fluid USP.

0724-8741/02/1000-1554/0 © 2002 Plenum Publishing Corporation

release dosage forms. For our purposes it is therefore critically important to identify a fluorophore that is sufficiently robust to allow accurate quantification of pH under these conditions.

In this paper, we attempt to fulfill these requirements by developing a CLSM method for quantification of pH, using a single water-soluble fluorophore that appears capable of operating under the conditions prevailing inside pellets containing 25% w/w of a soluble weak acid. In this initial paper, the method has been developed for mapping pH changes in uncoated extruded spheronised pellets and is utilised to compare pH changes in pellets containing two weak acid modifiers with different physicochemical characteristics. This method is a further contribution toward the development of techniques that may allow pharmaceutical scientists to better understand local processes within dosage forms (12, 25–27).

MATERIALS AND METHODS

Materials

Avicel PH101 (FMC; Cork, Ireland), fumaric and L-tartaric acid (Sigma Chemicals Co; Poole, Dorset, U.K.), and distilled water were used in pellet manufacture. Simulated intestinal fluid United States Pharmacopeia (USP) (29) without enzymes (SIF) was prepared using monobasic potassium phosphate and sodium hydroxide pellets (Sigma Chemicals; Poole, Dorset, U.K.). Rhodol Green carboxylic acid hydrochloride was obtained from Molecular Probes (Leiden, The Netherlands).

Preparation of Extruded and Spheronised Pellets

75g Avicel PH101 was dry mixed with 25 g weak acid modifier (fumaric acid or L + tartaric acid) in a K-blade planetary mixer at 60 rpm. 50mL distilled water was added to produce a wet mass that was then extruded through a Caleva model 10 extruder at 16 rpm. Forty-gram batches of extrudate were spheronised for 10 m at 1500 rpm in a Caleva model 120 spheroniser (Caleva; Sturminster Newton, U.K.). The pellets were dried for 12 h at 60°C and a 0.85–1.00 mm sieve fraction of pellets was used in the experimental work.

Confocal Laser Scanning Microscopy

Images were obtained using a Bio-Rad MRC-600 confocal laser scanning microscope (Bio-Rad Microscience; Hemel Hempsted, U.K.) equipped with a 15 mW Kr/Ar laser, attached to a Nikon Optiphot upright microscope with a x4, NA 0.13 objective and with settings of 0 neutral density, 0.2 confocal aperture. Under these conditions, the optical slice thickness was determined as approximately 50 μm. FITC/Texas Red filter blocks were used to obtain simultaneous images at Ex 488 nm/ Em 520 nm and Ex 568 nm/Em 580 nm. Individual images were captured as a 512 × 384 pixel array with each pixel coded 0–255 for intensity.

Fluorescent Response of Rhodol Green with Respect to pH and Concentration

Images of Rhodol Green solutions 1×10^{-3} to 5×10^{-5} g L^{-1} in SIF pH 7.5 at 37°C were used to establish the relationship between fluorescence and concentration. Rhodol Green solutions at pH 2.0–7.5 (adjusted with fumaric or tartaric acid) were imaged over the concentration range 1×10^{-3} to 2.5×10^{-4} g L^{-1} to determine the linear range of pH response. Fluorescence intensity was calculated as a mean pixel value over the whole image (n = 4), and these results were used to establish the mathematical model developed below, which allows calculation of pH values from the fluorescent intensity at Ex 488 nm and Ex 568 nm.

Confocal Microscopy Imaging of Hydrated Pellets

Pellets were hydrated in 2 mL of 2×10^{-3} gL^{-1} Rhodol Green in SIF at 37°C. At 5 min intervals the pellet was removed from the medium and placed under the confocal microscope on a microscope slide at 37°C. The plane of focus was moved by a downward stage traverse of 300 μm after focusing on the top of the pellet. On the same microscope slide, a 1 mm depth well containing 1×10^{-3} gL^{-1} Rhodol Green solution at pH 7.5 was used to standardise the emission intensity at Ex 488 nm and Ex 568 nm, and used to adjust each to a mean value of 224 pixel intensity. The pellet was then imaged at Ex 488 and Ex 568 nm, simultaneously. Under these conditions, the emission intensities from within the pellet represented the response at concentrations equivalent to 1×10^{-3} gL^{-1} Rhodol Green or below. Imaging was achieved typically in less than 1min. Between images, the pellet was returned to the medium. Measurements were made in triplicate.

Image Processing to Generate a Radial Profile of Fluorescent Intensity

A typical image pair is shown in Fig. 1 and image processing was undertaken using a macro written in Image Pro Plus v3 (Media Cybernetics LP; MD, USA). The stages in this procedure is illustrated schematically in Fig. 2. First, an outline of the edge of the pellet was obtained from the Ex 488 nm image. Then, by shrinking the initial outline shape of the pellet, the image was divided into a series of 3-pixel thickness concentric rings, and the mean pixel intensity was calculated for each ring from the number of pixels in the ring and the individual pixel intensities. The same procedure and ring pattern were used to delineate radial bands in Ex 488 nm and Ex 568 nm images and to obtain radial fluorescent intensity profiles from images at each time point. No discernible swelling or shrinkage of the pellets was observed during the experiments.

Concurrent Measurements of Internal Pellet pH Using a pH Microelectrode

A pH microelectrode with a 0.1 mm diameter metal-coated tip (World Precision Instruments; Stevenage, U.K.) was used to provide direct measurements of pH using sectioned pellets. In these experiments, the pellets were hydrated in 2×10^{-3} gL^{-1} Rhodol Green in SIF at 37°C, removed from solution, sliced through the center, and placed on a microscope slide at 37°C under the confocal microscope with the pH microelectrode touching the surface. Readings of pH could then be compared from measurements made simultaneously using the microelectrode and the fluorescence response from the area around the tip. A typical image from this experiment is shown in Fig.1b.

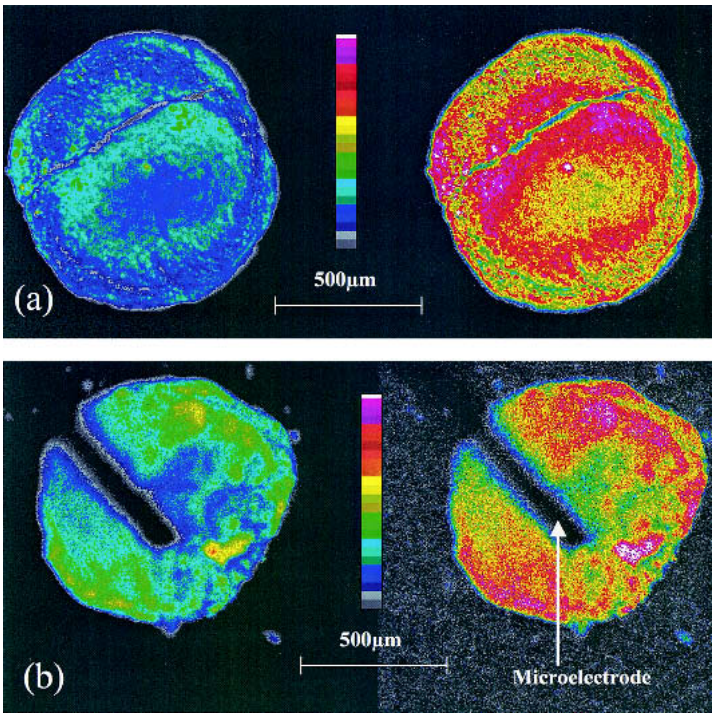

Fig. 1. Confocal fluorescence images obtained simultaneously at Ex 488 nm and Ex 568 nm from tartaric acid pellets hydrated for 10 min in $2 \times 10^{-3} gL^{-1}$ Rhodol Green in simulated intestinal fluid USP, pH 7.5 at 37°C. (a) Images obtained at a nominal depth of 300μm. (b) Images obtained from the surface of a sectioned pellet showing the microelectrode tip that is positioned flat on the surface. In both cases, the 488 nm image is left and the 568 nm image is on the right.

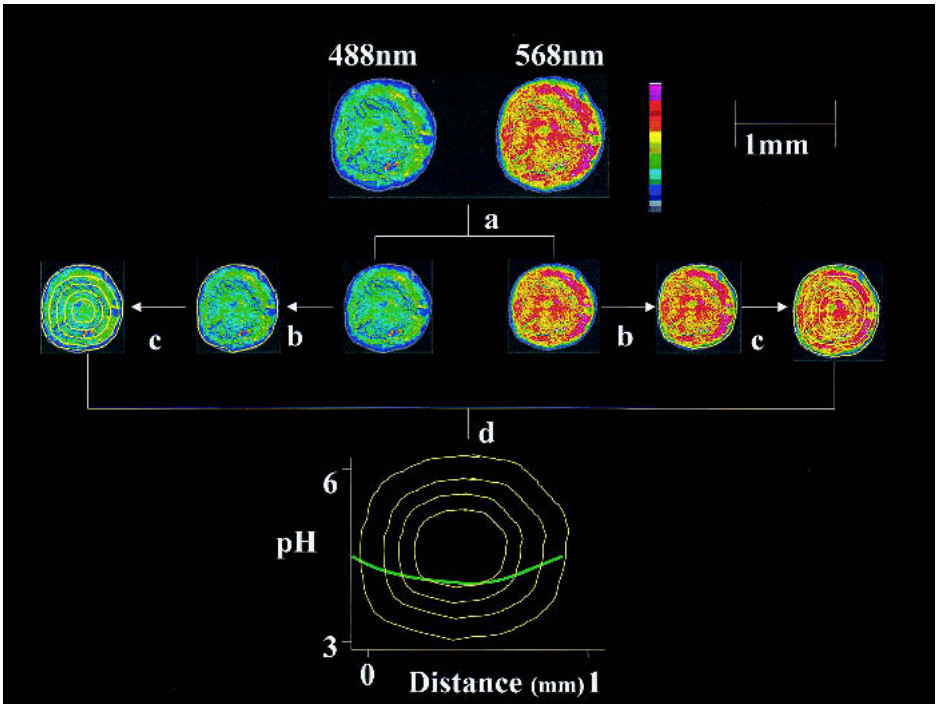

Fig. 2. An illustration of the image processing undertaken to generate a radially averaged pH profile from the confocal images. A dual image at Ex 488 nm (left) and Ex 568 nm (right) was generated for each time point. (a) The Ex 488 nm image was outlined. (b) And 3-pixel thickness rings were generated from the pellet outline. (c). The same template was applied to the Ex 568 nm image. Mean intensity values were calculated for pixels within each ring and converted to pH values using equation 5. The data was then represented as a graph. (d) This graph shows the pH value of each averaged ring as a function of distance from the pellet perimeter.

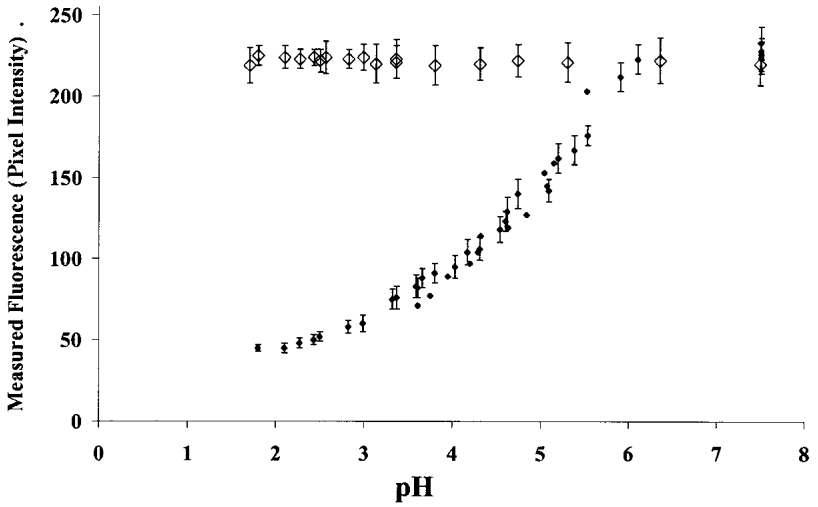

Fig. 3. The relationship between confocal fluorescent response and pH for 1x 10^{-3} gL^{-1} Rhodol Green solutions at Ex 488 nm *(solid diamond)* and Ex 568 nm *(open diamond)*. Each pint mean (n = 3) ± 1 SD.

RESULTS AND DISCUSSION

Deriving a Predictive Mathematical Model Relating Fluorescent Response, Concentration, and pH

A series of results are presented that describe the fluorescent response of Rhodol Green solutions at Ex 488 nm and Ex 568 nm with respect to concentration and pH, when imaged under the confocal microscope. At a given temperature and fixed depth of focus, a fluorophore with a pH sensitive response may exhibit changes in fluorescent intensity arising from changes in pH or in fluorophore concentration. For example, a low concentration response might occur in the early stages of dosage form hydration, and this will be indistinguishable from low pH unless there is an independent measure of fluorophore concentration. This can be provided by dual wavelength imaging as the fluorescent intensity of Rhodol Green is usually pH-dependent at Ex 488 nm but pH independent at Ex 568 nm. In this section, an experimental procedure and mathematic model is developed to test this assumption for solutions adjusted with tartaric and fumaric acid. Changes in fluorescence are quantified using the two measured values: $F_{488,}$ the measured emission intensity at Ex 488 nm, and $F_{568,}$ the measured emission intensity at Ex 568 nm, and interdependent relationships for fluorophore concentration and pH are obtained.

Fig. 3 shows the relationship between measured fluorescence and pH at $1 \times 10^{-3} gL^{-1}$, with the confocal microscope gain adjusted to equalise the fluorescence to a value of approximately 224 on a scale of 0–255 (pixel value) at both wavelengths at pH 7.5. At Ex 568 nm, the emission intensity remains at a constant value irrespective of pH whereas at Ex 488 nm, the measured emission intensity varies sigmoidally, reaching a maximum at pH 6. The graph demonstrates that under these conditions, (i) Rhodol Green response at Ex 488 nm was a good discriminator of pH over the range approximately pH 2 to 6 (ii) the response was pH insensitive at Ex

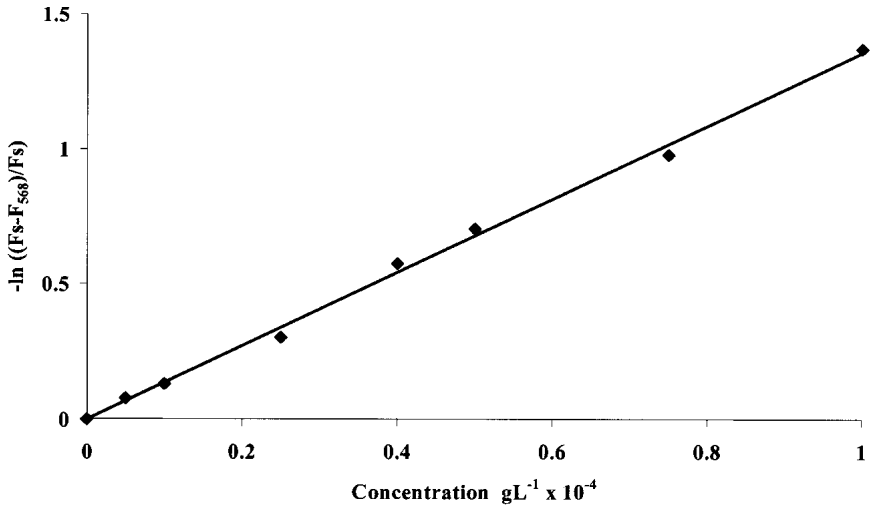

Fig. 4. The nonlinear relationship between fluorescent intensity and concentration at Ex 568 nm fitted to the exponential function of Eq. (2). Each point mean (n = 3).

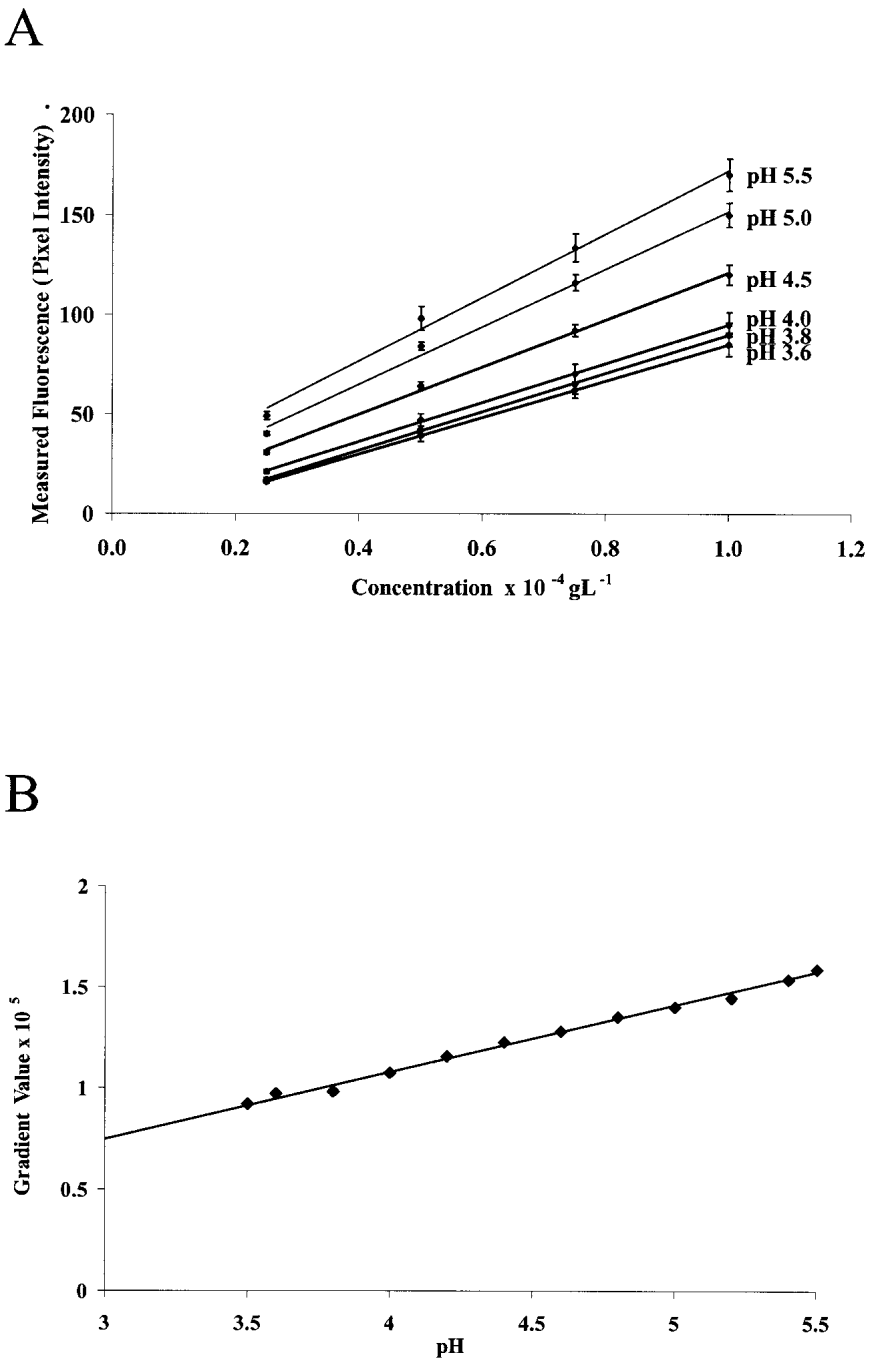

Fig. 5. (A) Graph shows how the linear dependence of fluorescent intensity on concentration is maintained over the full pH range of sensitivity at Ex 488 nm (each point mean n = 4 ± 1 SD). (B) Graph shows the linear relationship between pH and gradient values from Fig. 5a.

568 nm and may therefore be useful as an internal standard. Between pH 3.5 and 5.5 the response at Ex 488 was well approximated by a linear relationship ($r > 0.999$).

The pellet was hydrated using a fluorophore solution of at least 2×10^{-3} gL^{-1} . This ensured that there was sufficient fluorescence response from the pellet within a few minutes of hydration. This concentration provided a fluorescent response equivalent in intensity to a 1×10^{-3} gL^{-1} solution and compensated for attenuation of fluorescence by the pellet. The response at Ex 488 nm and Ex 568 nm was set using an external standard of 1×10^{-3} gL^{-1}. It was found that at Ex 568 nm the relationship between fluorescence and concentration was not linear .(Fig. 4) but followed an exponential relationship of the form;

$$F_{568} = Fs\,(1 - \exp(-\alpha C)) \quad (1)$$

where Fs is the saturated fluorescence level obtained at high concentrations, α is a parameter obtained from the data and C is the fluorophore concentration. Equation (1) can be inverted to give the following relationship for the fluorophore concentration;

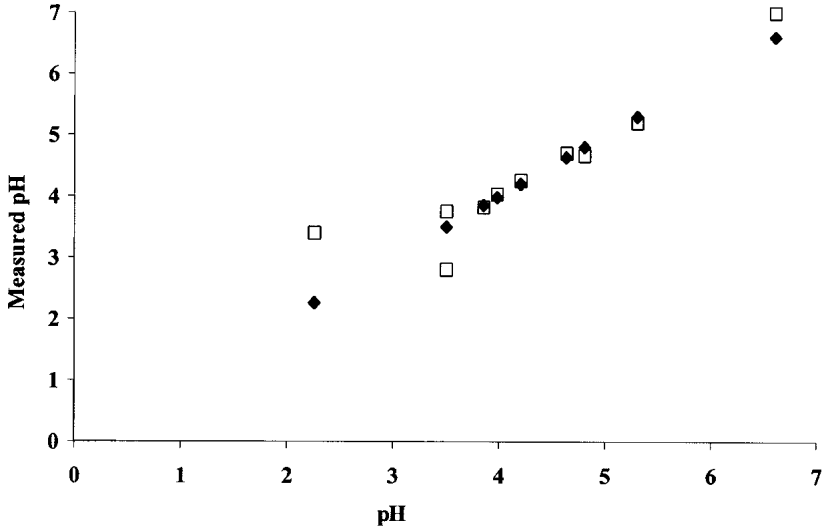

Fig. 6. Comparison of pH values obtained from fluorescence *(open squares)* and microelectrode *(closed diamonds)* measurements on the same hydrated tartaric acid pellets. Each value mean (n = 10).

$$C = [\ln Fs - \ln (Fs - F_{568})]/\alpha \quad (2)$$

and Fig. 4 shows a least squares fit of the data in Eq. (2), which yielded values of $Fs = 2.95 \times 10^2$ and $\alpha = 1.357 \times 10^3$ g L^{-1} (r = 0.999).

Fig. 5a shows how the fluorescent intensity at Ex 488 nm varies with both concentration and pH. Importantly, the concentration response remains linear at different pH levels within the range pH 3.5 to 5.5 and therefore at a given pH, the relationship between $F_{488,}$ the fluorescent intensity, and C, the concentration, is of the general form;

$$F_{488} = a_1 C + a_o \quad (3)$$

Both the gradient and the concentration axis intercept decrease with increasing pH, and a plot of gradient values a_1 against pH (Fig. 5b) shows that a strong linearity exists within the range of interest;

$$a_1 = b_1\, pH + b_o \quad (4)$$

A least squares fit of yields values of $b_1 = 33625$ and $b_o = -25250$ (r = 0.999) (Fig. 5b).

Rearranging Eq. (4) and substituting from equation 1 and 3 gives a predictive equation for pH in terms of the measured fluorescence intensities at F_{488} and F_{568}:

$$pH = \frac{-(F_{488} - a_0)\alpha}{b_1 \ln\left(1 - \frac{F_{568}}{F_s}\right)} - \frac{b_0}{F_s} \quad (5)$$

comparison of data values with the those predicted by Eq. (5), indicated errors of < 5% of the saturated fluorescence level. This ensures a minimum pH sensitivity of better than 0.5 pH units at the lowest measurable Rhodol Green concentrations. However, at the higher Rhodol Green concentrations encountered in the experiments, a pH sensitivity of 0.1 pH units would be typical. Solutions adjusted with fumaric and tartaric acid were found to exhibit the same relationship between fluorescent response, pH and concentration. To validate the pH values generated by the fluorescence model when used on pellets, a pH microelectrode was used to independently measure pH at the same time as fluorescence determinations were being made. The results are described below.

Images of Pellets Hydrated in SIF

Figure 1a shows images obtained from pellets taken after 10 min hydration in 2×10^{-3} gL^{-1} Rhodol Green in SIF at 37°C . The brightness of these images confirms that under these experimental conditions, sufficient fluorescent response was obtained within each image to be within the assay calibration. In addition, as the two images were superimposable when overlaid, wavelength dependent refraction is unlikely to be a significant factor in imaging of these samples. At zero time the images in Fig. 1 are of equal intensity, whereas after 10 min, there is an obvious decrease in intensity throughout the Ex 488 nm image; an apparent response of Rhodol Green to the dissolving tartaric acid.

Comparison of Fluorescence-Derived and Microelectrode Quantification of pH

Figure 1b shows images obtained with the pH electrode positioned on the surface of a sectioned tartaric acid pellet. pH values from the microelectrode were compared with those calculated using equation 5 from mean fluorescent intensity values in the region surrounding the electrode tip. Although the microelectrode only provides averaged values, the results (Fig. 6) show excellent correlation within the predicted range, and confirm pH 3.5–5.5 to be the effective range of Rhodol Green under these conditions.

Monitoring pH Change in Hydrated Fumaric and Tartaric Acid Pellets

The changing pH profile with time was monitored by generating a time sequence of image pairs at Ex 488 nm and Ex 568 nm, obtaining radial profiles by image processing, and applying equation 5 to generate graphs representing the spatial distribution of pH across the image.

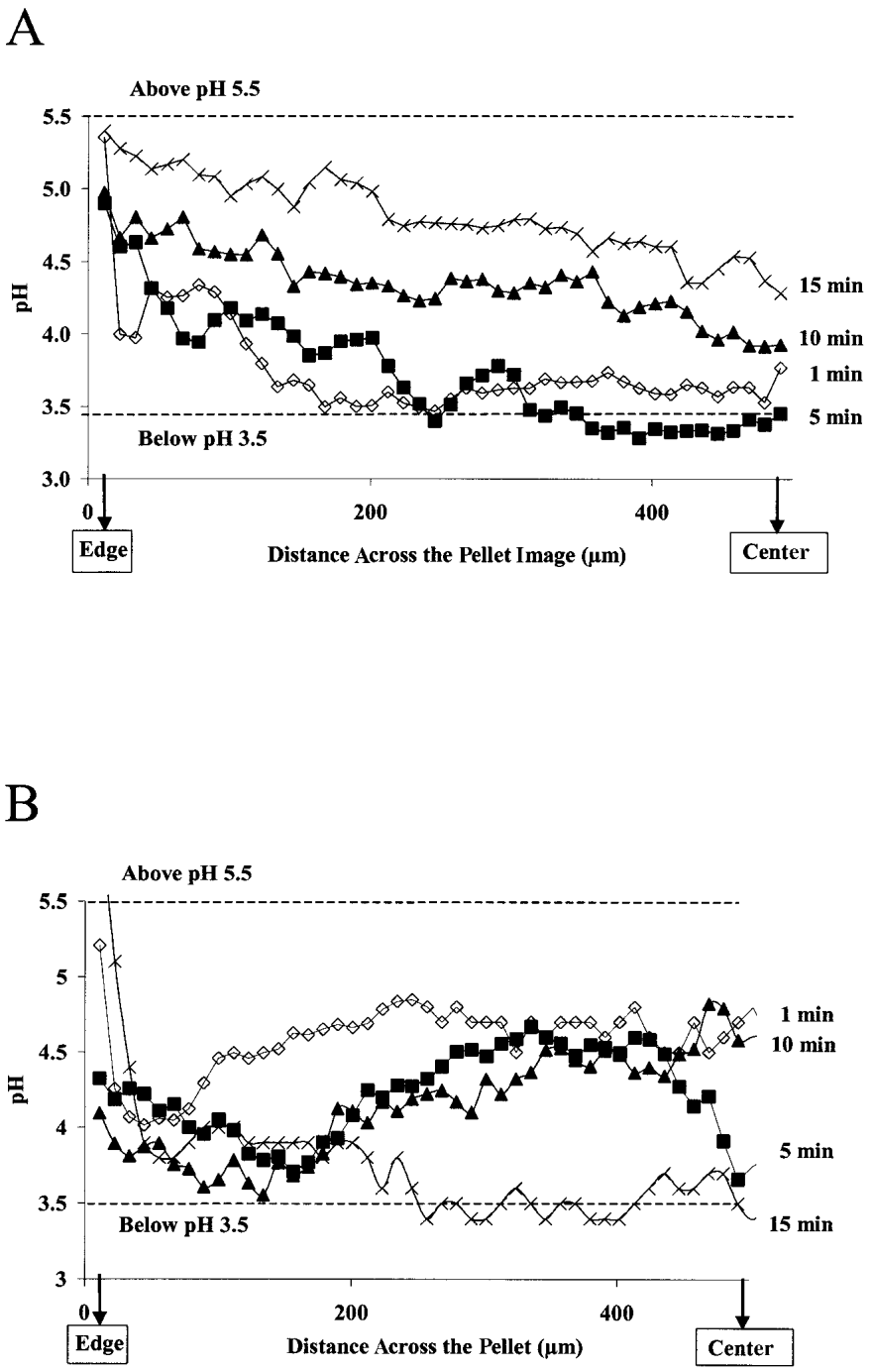

Fig. 7. The changing pH distribution obtained from images of a pellet in the early stages of hydration (A) tartaric acid and (B) fumaric acid pellets. Pellets were hydrated in 2×10^{-3} gL^{-1} Rhodol Green in simulated intestinal fluid USP, pH 7.5 at 37°C. The graphs show pH values between the edge and the center obtained for radially averaged bands obtained as in Fig. 2. Hydration time: *(open diamond)* 1 min, *(closed square)* 5 min, *(closed triangle)* 10 min, *(cross)* 15 min.

Fig. 7 and Fig. 8 show typical pH profiles from results repeated in triplicate. In the tartaric acid pellet images (Fig. 7a and Fig. 8a) the calculated pH dropped rapidly to values of 3.5 or less within 5 min of hydration. However, the low pH environment was maintained for only a short period; pH values were rising at 10 min, and at 20 min had reached pH 5.3 or above (Fig. 8a). In contrast, pH values calculated from fumaric acid pellet images (Fig. 7b and Fig. 8b) showed a slower onset of pH reduction but the maintenance of a low pH environment for a longer period. A minimum pH of 3.5–4.0 was achieved after 15 min, and pH 3.5 to 5.0 was maintained for at least 40 min after hydration (Fig. 8b).

The difference in this ability to create and maintain a low

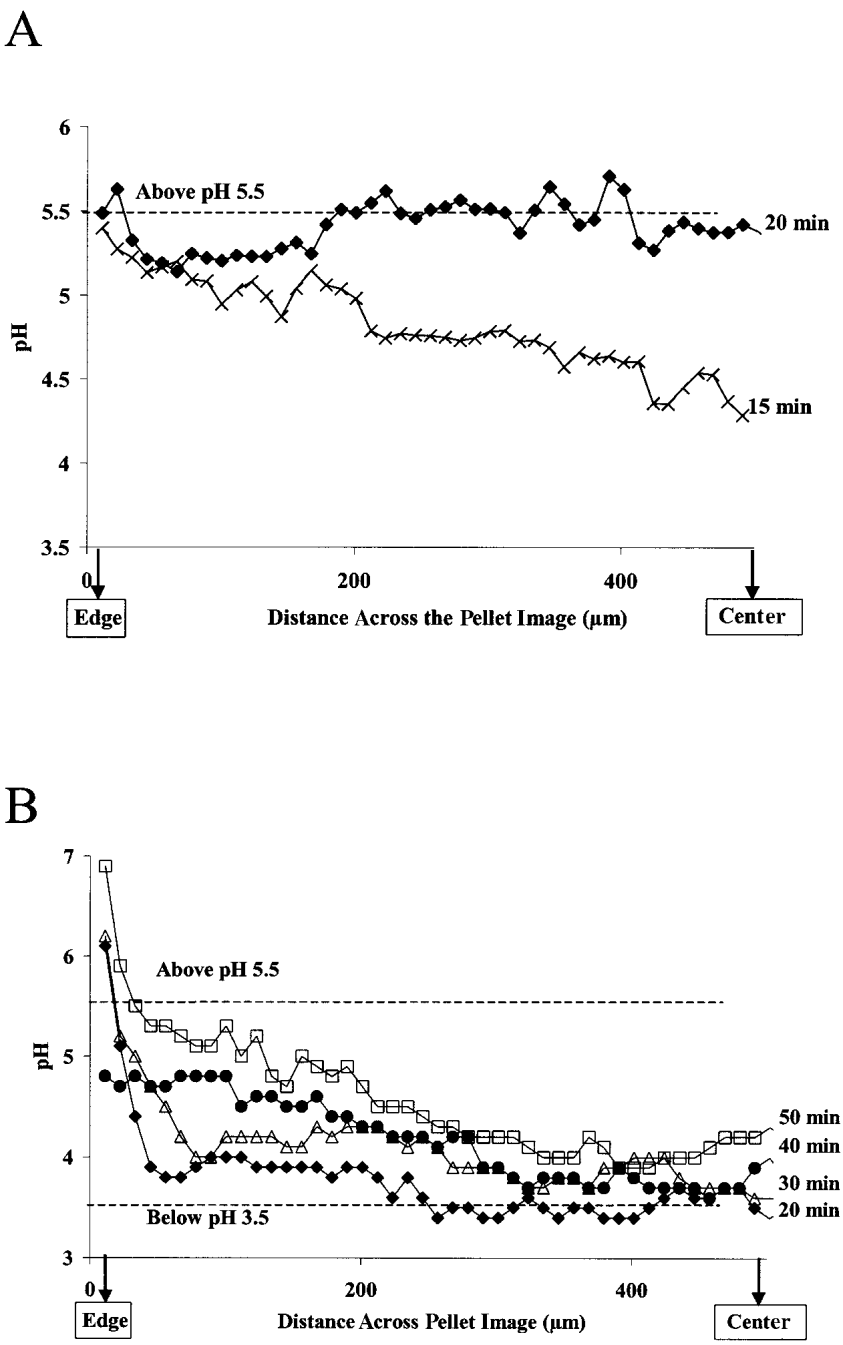

Fig. 8. The changing pH distribution in the later stages of hydration (A) tartaric acid (B) fumaric acid pellets. Hydration time *(cross)* 15 min, *(closed diamond)* 20 min, *(open triangle)* 30 min, *(closed circle)* 40 min,*(open square)* 50 min. Other details as Fig. 8.

pH environment may result simply from the physicochemical properties of the two acid modifiers. Fumaric and tartaric are both dicarboxylic acids with similar pK_a values (L-Tartaric: pK_1 2.98 pK_2 4.34. Fumaric: pK_1 3.03 pK_2 4.54 at 25°C)(29). However, they have very different water solubilities (L-Tartaric: 176g/100mL, Fumaric: 0.63g/100mL at 40°C) (29). It would therefore be reasonable to predict that the high solubility of tartaric acid would result in a rapid drop in pH, and the rapid attainment of a low pH environment, as was observed. However, complete dissolution of acid within a defined region of the pellet would also be achieved more quickly, and thereafter the low pH environment would deteriorate as the dissolved acid is lost from the pellet by diffusion. The result would be poor maintenance of pH as was observed in the results. In contrast, fumaric acid is much less soluble, and we might expect a less rapid drop in pH, and with lower saturation solubility, a higher pH environment. However, as the solubility is lower, fumaric acid may remain undissolved, and it may replenish acid lost by diffusion over a longer period. As a result the low pH within the pellet would be sustained. This is the pattern observed in these experiments.

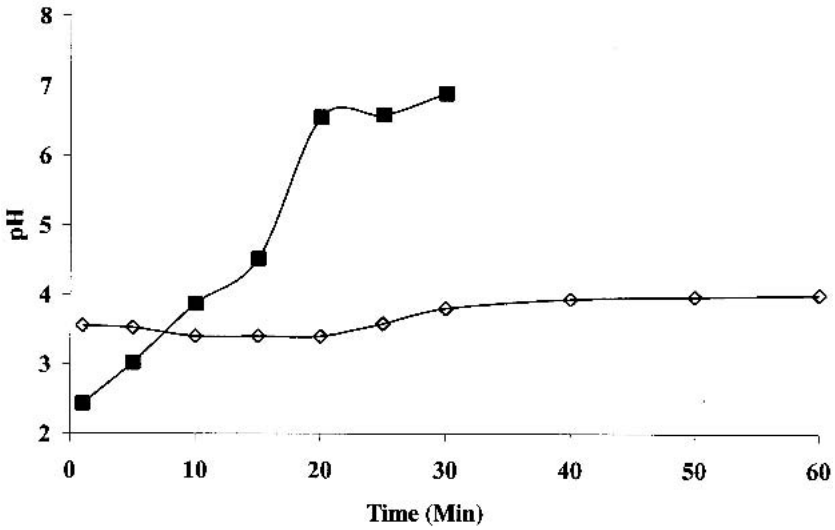

Fig. 9. pH values in sectioned tartaric acid *(closed square)* and fumaric acid *(open diamond)* pellets measured using the microelectrode method. Pellets were hydrated in simulated intestinal fluid USP, pH 7.5 at 37°C.

pH Change inside Weak Acid Pellets Measured Using the Microelectrode

Fig. 9 shows comparative results for sectioned fumaric and tartaric acid pellets measured using the microelectrode at different hydration times. In the tartaric acid pellets, the electrode detected a rapid drop to approximately pH 2.6 and a subsequent rise to pH 7 after 20 min hydration. In contrast, the pH within fumaric acid pellets reaches a minimum more slowly, but remains in the range pH 3.5 to 4.0 over the whole period. Given that the fluorescence assay cannot quantify pH outside the range pH 3.5 to 5.5, the closeness of this pattern to the time course profiles measured provides added confidence in the fluorescence determinations of pH.

CONCLUSIONS

This work provides a method for the noninvasive measurement and mapping of pH in an acid modified pharmaceutical pellet. Dual wavelength excitation and emission CLSM using the pH sensitive fluorophore Rhodol Green, appeared to be capable of accurately quantifying pH over the range pH 3.5 to 5.5 and monitoring the pH modifying behavior of tartaric and fumaric acids in uncoated pellets. The results correlate well with direct measurements of sectioned pellets made using a pH microelectrode. Whilst the microelectrode does allow determinations of pH outside the range of the fluorimetric method, it provides only averaged values, and the method is destructive as the pellet required cutting in half. In contrast, the fluorescence method developed here has the potential to provide spatially resolved information noninvasively, allowing time course experiments on the same pellet to be undertaken.

Under the conditions we examined, Rhodol Green appeared to be a robust indicator of pH within the environment generated by the hydrating pellet. While here, we have tailored the method to weak acids (pH modifiers suitable for solubility enhancement of weakly basic drugs) the approach is clearly generic and applicable to other dosage forms and pH ranges. This requires a fluorescent molecule to be identified that has (i) a pKa value in the range of interest; (ii) pH sensitive fluorescence at one wavelength; (iii) pH-independent fluorescence at a second wavelength that allows for correction of fluorophore concentration; (iv) these fluorescence responses to be capable of operating in the presence of high concentrations of soluble materials.

In summary, the approach provides a noninvasive method by which pharmaceutical scientists can monitor the changing pH environment in dosage forms and therefore provides a tool for optimising pH control.

ACKNOWLEDGMENTS

Thanks to Dr. Andy Billington (Datacell, U.K.) for writing the image analysis macro within Image Pro Plus; to Jonathan Sutch for help in verifying the mathematical model and with proofing; and to Pfizer Limited for funding of SJC.

REFERENCES

1. K. Thoma and T. Zimmer. Retardation of weakly basic drugs with diffusion tablets. *Int. J. Pharm.* **58**:197–202 (1990).
2. K. Thoma and I. Ziegler. The pH-independent release of fenoldopam from pellets with insoluble film coats. *Eur. J. Pharm. Biopharm.* **46**:105–113 (1998).
3. R. Bianchini, G.Bruni, A.Gazzaniga, and C.Vecchio. Influence of extrusion-spheronisation processing on the physical properties of *d*-indobufen pellets containing pH adjusters. *Drug Dev. Ind. Pharm.* **18**:1485–1503 (1992).
4. M. Kohri, N. Miyata, M. Takahashi, and H. Endo, K. Iseki, K. Miyazaki, S. Takechi, A.Nomura. Evaluation of pH-independent sustained release granules of dipyridamole by using gastric acidity controlled rabbits and human subjects. *Int. J. Pharm.* **81**:49–58 (1992).
5. G. M.Venkatesh. Development of controlled release SK & F 82526 J buffer bead formulations with tartaric acid as the buffer. *Pharm. Dev. Tech.* **34**:477–485 (1998).
6. C.Van Der Veen, H. Buitendijk, and C. F. Lerk. The effect of acidic excipients on the release of weakly basic drugs from the programmed release megaloporous system. *Eur. J. Pharm. Biopharm.* **37**:238–242 (1991).
7. K. E. Gabr. Effect of organic acids on the release patterns of weakly basic drugs from inert sustained release matrix tablets. *Eur. J. Pharm. Biopharm.* **38**:199–202 (1992).

8. N. Kohri, H.Yatabe, K. Iseki, and K. Miyazaki. A new type of pH-independent controlled release tablet. *Int. J. Pharm.* **68**:255–264 (1991).
9. C. Doherty and P. York. Microenvironmental pH control of drug dissolution. *Int. J. Pharm.* **50**:223–232 (1989).
10. C. Kroll, K. Mader, R. Stober, and H.H. Borchert. Direct and continuous determination of pH values in nontransparent w/o systems by means of EPR spectroscopy. *Eur. J. Pharm. Sci.* **3**:21–26 (1995).
11. K. Mader, S. Nitschke, R. Stosser, H. H. Borchert, and A. Domb. Nondestructive and localised assessment of acidic microenvironments inside biodegradable polyanhydrides by spectral spatial Electron Paramagnetic Resonance Imaging (EPRI). *Polymer.* **38**: 4785–4794 (1997).
12. L. S. Cutts, S. Hibberd, J. Adler, M. C. Davies, and C. D. Melia. Characterising drug release processes with controlled release dosage forms using the confocal laser scanning microscope. *J. Control. Release* **42**:115–124 (1996).
13. A. Shenderova, T. G. Burke, and S. P. Schwendeman. The acidic microclimate in poly(lactide-co-glycolide) microspheres stabilises Camptothecins. *Pharm. Res.* **16**:241–248 (1999).
14. K. Fu, D. W. Pack, A.M.Kilbanov, and R.Langer.Visual evidence of acidic environment within degrading poly(lactic-co-glycolic acid)(PLGA) microspheres. *Pharm. Res.* **17**:100–106 (2000).
15. R. Sanders, A. Draaijer, H. C. Gerritsen, P. M. Houpt, and Y. K. Levine. Quantitative pH imaging in cells using confocal fluorescence lifetime imaging microscopy. *Anal. Biochem.* **227**:302–308 (1995).
16. K. W. Dunn, S. Mayor, J. N. Myers, and F. R. Maxfield. Applications of ratio fluorescence microscopy in the study of cell physiology. *FASEB J.* **8**:573–582 (1994).
17. J. E. Whitaker, R. P. Haougland, and F. G. Prendergast. Spectral and photophysical studies of benzo[c]xanthene dyes: Dual emission pH sensors. *Anal. Biochem.* **194**:330–344 (1991).
18. P. N. Dubbin, S. H. Cody, and D. A. Williams. Intracellular pH mapping with SNARF - 1 and confocal microscopy. II: pH gradients within single cultured cells. *Micron.* **24**:581–586 (1993).
19. S. Bassnett, L. Reinisch, and D. C. Beebe. Intracellular pH measurement using single excitation - dual emission fluorescence ratios. *Am. J. Physiol.* **258**:171–178 (1990).
20. K. J. Buckler and R. D. Vaughan-Jones. Application of a new pH sensitive fluorophore (carboxy - SNARF - 1) for intracellular pH measurement in small, isolated cells. *Eur. J. Physiol.* **417**:234–239 (1990).
21. J. A. Thomas, R. N. Buchsbaum, A. Zimniak, and E. Racker. Intracellular pH measurements in Ehrlich ascites tumour cells utilising spectroscopic probes generated in situ. *Biochem.* **18**: 2210–2218 (1979).
22. Y. Zhou, E. M. Marcus, R. P. Haugland, and M.Opas. Use of a new fluorescent probe, seminaphthofluorescein-calcein, for determination of intracellular pH by simultaneous dual - emission imaging laser scanning confocal microscopy. *J. Cell Physiol.* **164**: 9–16 (1995).
23. J. Lui, Z. Diwu, and D. H. Klaubert. Fluorescent molecular probes III. 2′, 7′ - Bis - (3 - carboxypropyl) - 5 - (and - 6) - carboxyfluorescein (BCPCF): a new polar dual excitation and dual emission pH indicator with a pKa of 7.0. *Bioorg. Mel. Chem. Lett.* **7**:3069–3072 (1997).
24. S. Mordon, J. M. Devoisselle, and S. Soulie. Fluorescence spectroscopy of pH in vivo using dual - emission fluorophore (C - SNAFL - 1). *J. Phytochem. Photobiol. B: Biol.* **28**:19–23 (1995).
25. L. S. Cutts, P. A. Roberts, J. Adler, M. C. Davies, and C. D. Melia. Determination of localised diffusion coefficients in gels using confocal scanning laser microscopy. *J. Microscopy* **180**:131–139 (1995).
26. C. D. Melia, A. R. Rajabi-Siahboomi, A. R. and R. W. Bowtell. Magnetic resonance imaging of controlled release pharmaceutical dosage forms. *Pharm. Sci. Tech. Today* **1**:32–39 (1999).
27. J.Adler, A.Jayan, and C. D. Melia. Quantifying differential expansion within hydrating hydrophilic matrices by tracking embedded fluorescent microspheres. *J. Pharm. Sci.* **88**:371–377 (1999).
28. *United States Pharmacopoeia* 24. United States Pharmacopeial convention. 1999.
29. S. Budavari. Ed. *The Merck Index. Twelfth Edition.* Merck & Co Inc, New York, 1996